Ecological Indicators 144 (2022) 109520

Contents lists available at ScienceDirect

Ecological Indicators

journal homepage: www.elsevier.com/locate/ecolind

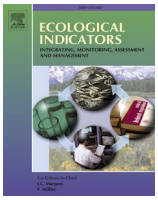

Habitat compression indices for monitoring ocean conditions and ecosystem impacts within coastal upwelling systems

Isaac D. Schroeder [a,b], Jarrod A. Santora [c,d,*], Nate Mantua [c], John C. Field [b,c], Brian K. Wells [c], Elliott L. Hazen [a,b], Michael Jacox [a,b], Steven J. Bograd [a,b]

[a] Environmental Research Division, Southwest Fisheries Science Center, National Marine Fisheries Service, National Oceanic and Atmospheric Administration, Monterey, CA 93940, United States
[b] Institute of Marine Sciences, University of California, Santa Cruz, CA 95060, United States
[c] Fisheries Ecology Division, Southwest Fisheries Science Center, National Marine Fisheries Service, National Oceanic and Atmospheric Administration, Santa Cruz, CA, United States
[d] Department of Applied Math, University of California, Santa Cruz, CA, United States

ARTICLE INFO

Keywords:
Thermal habitat
Ecosystem shift
Marine heatwave
Fishery patterns
Upwelling ecosystems

ABSTRACT

Upwelling ecosystems are characterized by intense seasonal productivity that supports highly dynamic species populations, high diversity of mid and upper trophic levels, and a myriad of important fisheries. Climate variability and long-term change will impact upwelling intensity, timing and persistence, thereby potentially threatening resilience of coastal food webs and stability of ecosystem services. The spatial footprint of cool upwelled waters in the surface mixed-layer supports trophic transfer and ultimately the productivity of fisheries. The spatial area of upwelled water in eastern boundary upwelling systems can vary dramatically in response to both local and remote atmospheric forcing. These variations contribute to dynamic habitats that impact the structure, function, and spatial characteristics of marine ecosystems. We quantified the variability in "cool-water thermal habitat" area as a new ecological indicator, the Habitat Compression Index (HCI), for the nearshore (within 150 km of the coast) waters of the California Current Large Marine Ecosystem (CCLME). The HCI can be easily updated from ocean model products and satellite observations of sea surface temperature. We describe standardization of the HCI, regional variability, and evaluate HCI relationships with other indicators commonly used to inform ecosystem context within the CCLME. Importantly, our approach to calculating the HCI is easily extendable to other upwelling ecosystems. Further, we discuss the management context of the HCI such as assessing risk of whale entanglement in a highly profitable fishery, and implications for monitoring ecosystem shifts in coastal upwelling systems and the fisheries they support.

1. Introduction

Eastern Boundary Upwelling Systems (EBUS) are among the most productive marine ecosystems in the world, supporting some of the largest fisheries (Chavez and Messié 2009, Kampf and Chapman 2016, Checkley et al. 2009). In the California Current Large Marine Ecosystem (CCLME), the EBUS off the west coast of North America, coastal upwelling plays a critical role in providing nutrients essential for primary productivity and population growth of secondary and tertiary consumers, that extends from mid-water to benthic species, as well as attracting highly migratory air-breathing predators (Block et al. 2011). The spatial extent of cool upwelling habitat varies temporally and spatially within the CCLME and has consequences for the distribution and aggregation of planktonic organisms, production and distribution of coastal pelagic species, their predators and socio-economics of important fisheries. These changes in upwelling habitat occur on sub-seasonal to interannual and decadal scales, and are understood to influence ecosystem productivity (Hubbs 1948, Parrish et al. 1981, Chavez et al. 2003, Di Lorenzo et al., 2013). Climate change is expected to have substantive impacts on upwelling ecosystems above and beyond their historical scope of variability, as a result of changes in a suite of complex and interacting factors including wind stress and upwelling intensity, ocean acidification, changes in source waters and changes in the magnitude and frequency of extreme events (Bakun et al. 2015). For

* Corresponding author.
E-mail address: jarrod.santora@noaa.gov (J.A. Santora).

https://doi.org/10.1016/j.ecolind.2022.109520
Received 8 May 2022; Received in revised form 27 September 2022; Accepted 29 September 2022
Available online 10 October 2022

example, the development and multi-year persistence of large marine heatwaves (MHWs) are new and emerging events that impact marine ecosystems and fisheries that depend upon them. During the 2014–2016 Northeast Pacific MHW, warm oceanic waters expanded into the near-shore CCLME, compressing the spatial extent of cool upwelled water and thus the available habitat space for coastal ecosystem processes to take place (Santora et al., 2020). This MHW and compression of cool-water habitat was associated with ecosystem shifts, a toxic algal bloom and changes in coastal species assemblages of predators and prey (Cavole et al. 2016, Santora et al. 2020), which together contributed to severe impacts on socio-economic systems, including fisheries (Ritzman et al. 2018; Holland and Leonard 2020; Samhouri et al. 2021). To better prepare for future threats to marine life and fisheries posed by ocean warming, we need ecologically meaningful indicators that communicate dynamic shifts in pelagic habitat.

In the CCLME, ocean climate indices (e.g., indicators for the El Niño/Southern Oscillation (ENSO), or the Pacific Decadal Oscillation (PDO) are monitored to track ocean basin-scale patterns of cool and warm ocean surface temperature regimes that relate to ecosystem productivity patterns (Peterson et al. 2014; Schroeder et al. 2014). Ocean climate indices can be derived from gridded sea surface temperature (SST) fields, and can be provided as time series reflecting averages or anomalies over broad regions or entire ocean basins. Although EBUSs are influenced by ocean basin-scale processes, they are also responding to localized ocean circulation patterns and wind stress, and the spatial extent of cool-water habitat generally reflects the spatial extent and distribution of high primary and secondary productivity that is favorable for many higher trophic species in the CCLME (Santora et al. 2021). Therefore, area-based time series of thermal habitat may provide rapid assessment of habitat suitability impacted by climate variability and change that broad scale indices may not capture. We refer to the normalized area of "cool-water" thermal habitat within an upwelling ecosystem as the habitat compression index (HCI).

Here we develop the HCI as a regional-scale indicator for informing dynamic ocean management (Maxwell et al. 2015; Santora et al. 2020), constructed to describe the area of cool waters over the coastal-pelagic habitat along the continental shelf of the CCLME. As thermal regimes and coastal upwelling processes vary geographically throughout the CCLME, we describe and discuss the use of four regional HCIs within the CCLME. Output from a data-assimilative regional ocean circulation model (combined historical reanalysis and near real time models; Moore et al. 2011, Neveu et al. 2016) is used to develop the HCI. To benefit replication in ecosystems without operational regional ocean models, we show how the HCI may be easily calculated from standard gridded SST fields. We also show that cool-water habitat indexed by the HCI extends to the mixed layer and is not just a surface feature.

Historically, regional upwelling and the basin-scale SST-based PDO index have been two main indicators used to inform ecosystem productivity in the CCLME (Weber et al. 2021). For example, traditional upwelling indices and estimates of nutrients upwelled in the water column are used to examine variability (daily to interannaual) and non-linear relationships between winds and Chl-a production (Jacox et al. 2016, 2018). In contrast, the PDO index is resolved monthly and represents basin-spatial scale fluctuations of North Pacific thermal habitat, including that in the eastern North Pacific Ocean (Mantua et al. 1997), and informs potential changes in marine species productivity and distribution (e.g., copepods and salmon – Peterson et al. 2014; Sardines and Anchovies – Chavez et al. 2003). During the 2014–2016 MHW, wind-based upwelling indices were close to average within the CCLME, yet the offshore extent of cool upwelled water was highly compressed along the coast, resulting in marked changes in pelagic species distributions (Santora et al. 2017, 2020). Therefore, the HCI may better capture variability of temporal and spatial extent of cool water conditions than basin-scale indicators like the PDO index, and inform regional variability of marine ecological structure. In this study, we explore this concept by comparing the HCI with the PDO and upwelling indices, and with micronekton species abundance, distribution and biodiversity indices (Santora et al. 2017, 2021a). Ecological productivity has been hypothesized to vary regionally based on the cumulative sum of upwelling from the winter into the spring upwelling season (Schroeder et al. 2013; Wells et al. 2017; Santora et al. 2021a). As a CCLME application, we examine whether the HCI or standard regional indices (e.g., upwelling and sea level) during the winter correlate more strongly with abundance and variability of krill, anchovy and pelagic biodiversity during the spring at regional scales.

Ecological indicators should be straightforward to interpret, have clear thresholds, and be easy to monitor in near real time to inform rapid assessment of environmental changes within an ecosystem (Rice and Rochet, 2005). Communication of ecosystem indicator status is further strengthened if it is easily translated to a diverse group of stakeholders, especially in complex socio-economic systems like fisheries that involve management of living marine resources and human activities. In that regard, the HCI provides ecosystem context that, combined with basin-scale climate indices, offers a regionalized index for monitoring coastal thermal habitat associated with coastal pelagic ecosystem shifts. We discuss the application of the regional HCI for communicating ecosystem context for mitigating risk of whale entanglement in fixed gear fisheries, and potential challenges arising from impacts of ephemeral events such as MHWs. Finally, we describe a web-based tool for viewing monthly spatial and temporal habitat compression patterns in the CCLME.

2. Methods

2.1. Regional ecosystem indicator context

Upwelling onset and intensity vary greatly over the CCLME (Bograd et al 2009), with bathymetric and orographic features influencing upwelling and oceanic currents (Hickey 1998, King et al. 2011, Ware and Thomson 2005). Points and capes can locally intensify upwelling and submarine canyons can be conduits for subsurface nutrients into the surface layer (Hickey and Banas, 2008). Regional differences in geographic features, canyons, and oceanic features result in contrasting ecosystem states that can be thought of as unique biogeographic provinces (Checkley and Barth, 2009; Table 1). Each of these regions also have unique epipelagic species assemblage, abundance and diversity patterns (Peterson et al. 2013; Ralston et al. 2015; Friedman et al. 2018). For regional fishery and ecosystem management context, the CCLME between 30 and 48°N is presented here as 4 biogeographical regions that extend south to Baja California (Table 1; Supplemental Fig. S.1). We chose to place the boundaries of these regions either to the north or south of major coastal promontories to account for the location of strong upwelling centers and retention zones both upstream and downstream. For example, boundaries are not placed directly at Cape Blanco, Cape Mendocino, or Point Conception, because upwelling centers would be cut in half and effects of retention to the north/south of these regions would likely misrepresent the extent of habitat compression dynamics within and among regions (for location of strong upwelling winds see Supplemental Fig. S.1). The 150 km offshore extent of the regions covers continental shelf and slope habitats, and is predetermined to account for the extent of upwelling habitat and influence of offshore oceanic waters (Jacox et al. 2018) (Fig. 1a). Over a majority of the CCLME the shelf is within 75 km of the shore (excluding islands, see red line Fig. 1a). This 75 km offshore extent is a region of positive vertical velocities (upwelling) and higher nitrate and chlorophyll concentrations during the climatological upwelling season (Jacox et al. 2016). In addition to strong latitudinal changes in sea surface temperature, there are gradients in wind forcing, with generally greater seasonality to wind stress and primary/secondary productivity in northern regions and weaker seasonality in the southern regions.

Table 1
The four Habitat Compression Indices describe the area of cool water in unique biogeographical provinces in the California Current Large Marine Ecosystem. The area of cool water is calculated for regions between the latitudinal ranges (Latitude Range column) and from the shore out to 150 km.

	Latitude Range	Geographic Features	Canyons	Oceanic Features
Region 1	48 to 43.5°N	• Juan de Fuca/ Columbia River • Relatively smooth coastline, wider shelf in the north	Several large canyons	• Upwelling and freshwater plumes interaction • Summer hypoxic events
Region 2	43.5 to 40°N	Large coastal promontories (Cape Blanco in the north and Cape Mendocino in the south)	Many small canyons	• Strong upwelling at capes • Retention between the capes
Region 3	40 to 35.5°N	• Smaller coastal promontories (Points Arena and Reyes) • San Francisco and Monterey Bays	• Monterey Bay Canyon • Extensive canyon habitat	• Strongest upwelling at Point Arena • Retention in Gulf of Farallones and Monterey Bay
Region 4	35.5 to 30°N	• Point Conception headland • Southern California Bight • Channel Islands • Offshore basins	No canyons	• Strong upwelling at Pt Conception • Retention in the bight

2.2. Oceanographic model output

The regional HCIs use 2 m temperature (T_{2m}) data from two complimentary data-assimilative oceanic models of the CCLME (https://oceanmodeling.pmc.ucsc.edu/, Moore et al. 2011, Neveu et al. 2016). The models assimilate in situ hydrographic data and satellite observations for high spatial resolution on sub-daily time scales, providing an effective interpolation framework of sparse hydrographic observations or missing satellite temperature observations due to cloud coverage. Two time periods are included in this study, a 31 year period over 1980 to 2010 and a 10 year period from 2011 to December 2020. The model covering 1980–2010 is called WCRA31 and the model from 2011 to 2020 is called the Near Real Time (NRT). The NRT is updated daily and the output is served operationally by UCSC (oceanmodeling.ucsc.edu). The surface-oriented temperature data served by Central Northern California Ocean Observing System (CeNCOOS; https://www.cencoos.org/) is on standard depths of 2, 5, 10, 20, 40 m and every day a run is performed over the preceding four days and estimates are made available on the CeNCOOS data portal. Offshore in deeper water (e.g., 4000 m) there are no temperature data at 2 m due to the conversion between the 42 sigma levels to actual depth levels. In the situation where a temperature profile is missing 2 m values the available profile is extrapolated to the 2 m level using the *scipy.interpolate.interp1d* routine in Python 3.6.

Surface temperatures are consistent between the two models and have been integrated through time in ecological studies investigating marine species distributions (Becker et al. 2016; Brodie et al. 2018; Abrahms et al. 2019; Cimino et al. 2020). However, temperature data below 2 m depth can have biases between the two models (Neveu et al. 2016; Brodie et al. 2018), consequently all subsurface temperature data used in this analysis consists of output from the WCRA31 model for 1980 to 2010 to avoid consistency issues. Subsurface analysis is used for model evaluation purposes but is not needed for real-time HCI calculation.

Temperature data is extracted from model output based on the distance from shore. Two distance from shore masks were created: a 75 km mask was used for identifying monthly thresholds and a 150 km mask for calculating the HCI. The distance from shore mask is created from the ROMS land mask file, which distinguishes all grid points as either water or land. The distance from shore masks are created by finding all grid points that are located 75/150 km from any coastal edge land grid points, excluding islands.

2.3. Habitat compression Index

The HCI is resolved on monthly scales and monthly means of T_{2m} are created from daily output from WCRA31 and NRT models. There are 2 steps to the calculation of a regional HCI: 1) establish 31 year (1980–2010) climatological monthly temperature thresholds and 2) estimate the area of T_{2m} in each region that falls below that region's climatological monthly temperature threshold for each month. Climatological monthly thresholds are needed in each region to account for seasonal and meridional temperature differences in the regions (Huyer 1983; Hickey et al. 1998). The first step uses temperature data over a climatological time period (1980–2010). This allows for temperature thresholds to be calculated once and avoids recalculating thresholds when the temperature dataset is updated with new monthly means. Importantly, with secular ocean surface warming trends expected to continue, baseline periods will need to be reevaluated and updated in the future (Xiu et al. 2018).

All T_{2m} time series at grid locations within a region up to 75 km offshore are spatially averaged to obtain one time series for the region. A monthly mean climatology for the region is calculated from this time series by averaging all values for a given month over the 1980–2010 time period. The monthly values are rounded to the nearest half-degree and represent temperature thresholds for calculating the HCI for each region (Fig. 2a). The second step is done for every month from 1980 to present and results in a time series of monthly areas - this is the HCI time series. The monthly areas are the sum of all grid-point areas in each region (within 150 km of shore) that fall below the monthly threshold normalized by the total area of the region (Fig. 2b). This normalization enables comparison of HCIs across regions and across EBUSs. The resulting HCI has a minimum of 0 (no cool-water habitat) and a maximum monthly value of 1 (cool habitat over the entire region). For the full time series, the mean and $\pm$ 1 standard deviation, provides a quick reference for inferring low, medium and high compression states.

Upwelling conditions and spatial extent of cold water can vary substantially at monthly scales (Jacox et al. 2018). We present a diagnostic tool for monitoring progression of the HCI within each region to track changes in the HCI and provide comparison among years. For example, this allows comparison of how the HCI varies during periods characterized by anomalously warm and cool conditions. The progression of HCI values over a yearly interval is analyzed by constructing a cumulative HCI curve for a given year. The yearly cumulative curve is the sum of all yearly values over January to December within that year. Since the monthly HCI has a maximum value of 1, the cumulative sum ending in December can be a maximum of 12. The cumulative HCI is comparable to the cumulative upwelling index (CUI) and provides a similar indicator of sustained physical conditions on ecosystem productivity (Bograd et al. 2009).

Although the ocean model assimilates satellite observations, it is still important to compare HCIs derived from the model and other gridded SST products. This is because direct computation from gridded SST fields offers an alternative source for updating HCI values for operational purposes. Further, we recognize that regional data-assimilative ocean models are not available in all parts of the world ocean, so demonstration of the index using existing publicly available gridded SST fields will benefit those needing to monitor habitat compression in other marine ecosystems. As a validation of T_{2m} output from the ROMS models, the regional HCI is compared to indices constructed from NOAA's Optimal

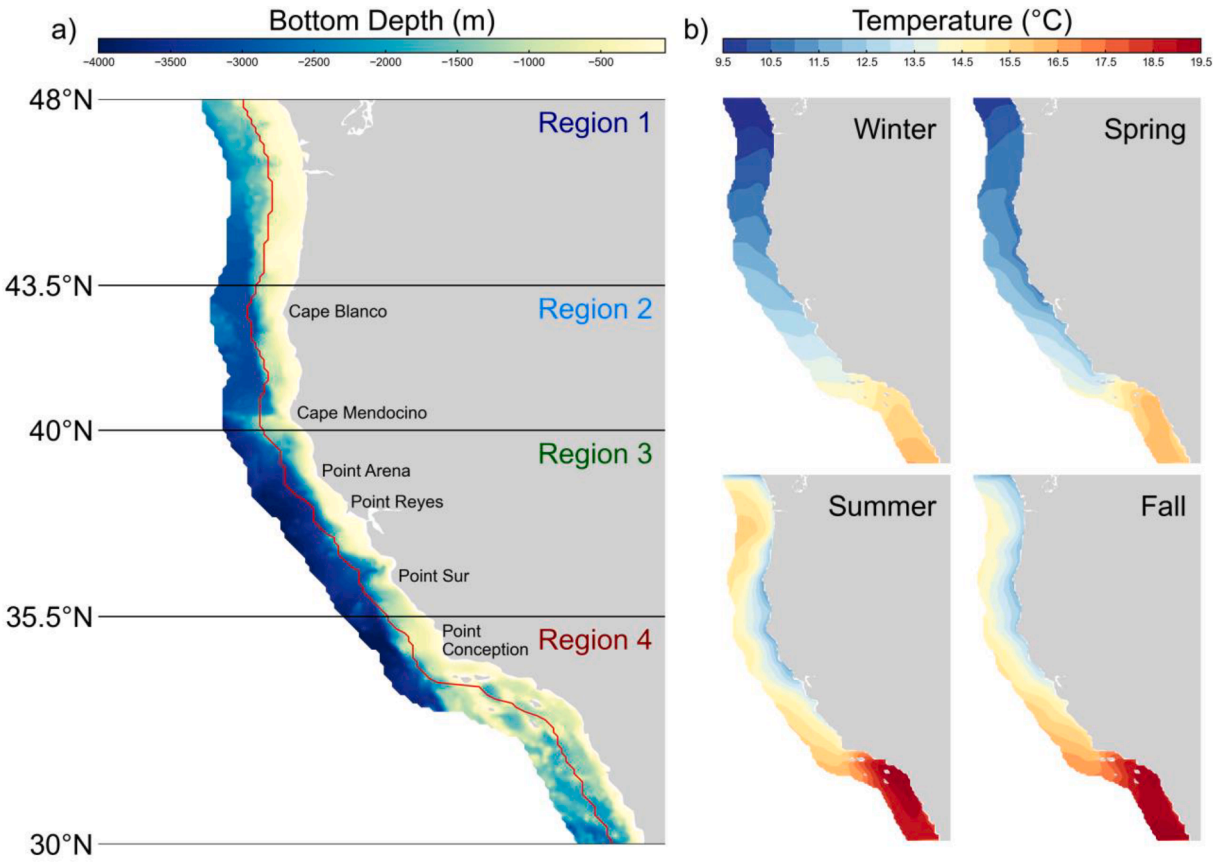

Fig. 1. Geography, bathymetry and seasonal sea surface temperature climatologies for the California Current Large Marine Ecosystem: (a) bottom depths out to 150 km from the coastline; this area consists of the continental shelf, slope, and submarine canyons. The four regions mark biogeographical provinces where Habitat Compression Indices (HCI) are calculated. The red line equidistant to the coast is 75 km from shore (excluding islands), and this area is used in defining monthly thresholds required in calculating the HCI. (b) Seasonal climatology of sea surface temperatures. The climatology was constructed from 2 m temperature time series extracted from a data-assimilative ROMS over 1980 to 2010. (For interpretation of the references to color in this figure legend, the reader is referred to the web version of this article.)

Interpolated SST that is based on satellite, ship, buoy and Argo float observations (Huang et al. 2020). We also analyzed temperature data at various depths to verify the consistency in HCI at selected depths between 2 and 40 m.

2.4. Comparison to environmental and ecological indicators

The HCI is compared to basin-scale indices that reflect environmental conditions in the Northeast Pacific (PDO Index; North Pacific Gyre Oscillation, NPGO Index) and the tropical Pacific (Oceanic Niño Index, ONI), and indicators of regional conditions (e.g., sea level height and coastal upwelling). The PDO Index (Mantua et al. 1997), ONI (metadata found at https://origin.cpc.ncep.noaa.gov/) and NPGO Index (Di Lorenzo et al. 2008) are monthly resolved with data lengths longer than the HCI. Sea level was derived from 4 coastal tidal gauges (9435380 South Beach, OR; 9419750 Crescent City, CA; 9414290 San Francisco, CA; 9410170 San Diego, CA) that have measurements before 1980, with one contained in each HCI region. The monthly tidal gauge data was downloaded from https://tidesandcurrents.noaa.gov/, which provided monthly mean sea level (Monthly_MSL) and an estimated long-term trend (Linear_Trend) (see Sweet et al. 2017 and reference within); for this analysis detrended time series were constructed by subtracting the long-term trend from the monthly mean sea level. The Coastal Upwelling and Transport Index (CUTI) and Biologically Effective Upwelling and Transport Index (BEUTI; Jacox et al. 2018) are an estimate of coastal upwelling at 1° intervals between 31 and 47°N, with CUTI providing estimates of nearshore vertical transport and BEUTI estimates of nearshore vertical nitrate flux. Region specific CUTI and BEUTI time series were created by averaging all 1° CUTI or BEUTI time series within each of our four regions. From the northern CCLME, the Northern copepod biomass anomaly (monthly observations since 1996; from monitoring off Newport, OR), is an indicator for the transport of subarctic waters into the northern CCLME, as northern copepods originate from the Gulf of Alaska (Peterson and Miller, 1975; Fisher et al., 2015). All monthly time series were examined for seasonality and anomaly time series were created by subtracting the monthly climatological value for a given month. Anomaly time series for the correlation analysis had linear long-term trends removed by least-square regression. Comparison between these indices and HCIs were done using Spearman's rank correlations and significance was determined at $p < 0.01$.

Additional ecological evaluation of the HCI is made by comparison with a subset of indicators known to vary with changes in ocean and climate dynamics that in turn provide context on ecosystem function and state (Peterson et al. 2013; Santora et al. 2017, 2021a, b). Ecological connections with the HCI are presented for evaluating and refining hypotheses pertaining to mechanisms impacting ecosystem structure (Santora et al. 2021a). For this evaluation, ecological data is used from the Rockfish Recruitment and Ecosystem Assessment Survey (RREAS), which has the longest sampling history within Region 3. The RREAS monitors epipelagic micronekton using a mid-water trawl towed for 15 min targeting a 30 m headrope depth; Sakuma et al. 2016; Santora et al. 2021). We focus on the long-term time series from a subset of consistent sampling of 34 stations within the Greater Gulf of the Farallones and Monterey Bay (between 36.6 and 38.2°N) in late spring (May-June).

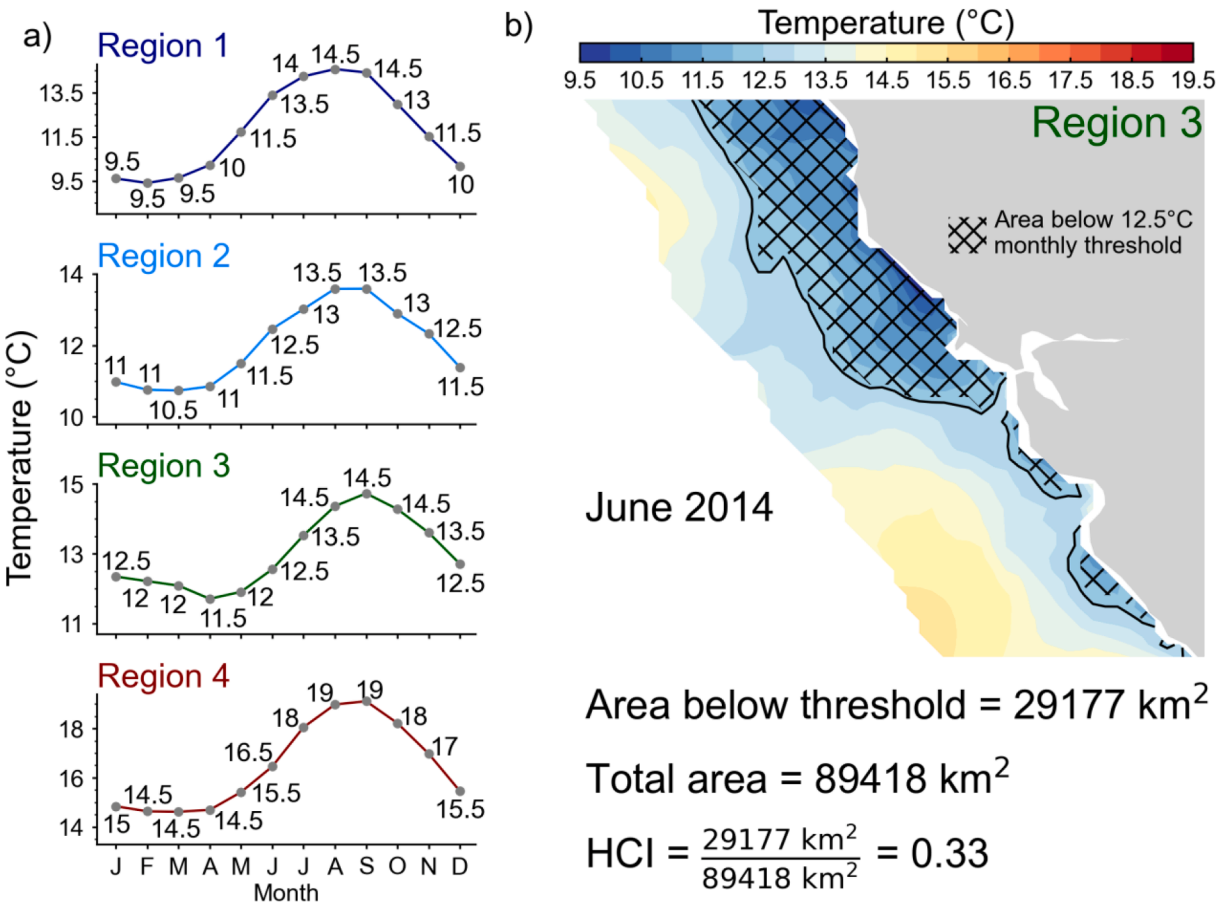

Fig. 2. Graphical illustration example on how the Habitat Compression Index is calculated based on temperature thresholds: (a) Monthly climatologies and temperature thresholds used for the four Habitat Compression Indices. The monthly climatology (solid lines and circles) are derived from monthly time series (1980–2010) of spatially averaged temperatures at 2 m over the region's latitude range and extending out to 75 km from shore. The labeled temperature thresholds are the corresponding monthly climatological value rounded to the half degree. (b) An example HCI calculation for Region 3 on June 2014. The contour is the monthly mean of surface temperatures extending out to 150 km from the shore. The HCI value is the area below the 12.5 °C June temperature threshold normalized by the total area of the region.

Most species encountered by the survey have been identified and enumerated for every net trawl conducted since 1990, allowing for abundance estimates based on catch per unit effort (CPUE) and calculation of biodiversity metrics such as Shannon-Weaver Diversity (Santora et al. 2017). Time series of krill and anchovy abundance were developed based on generalized linear models as in Santora et al. (2021b), while diversity indices are updated based on methods in Santora et al. (2017).

We compare the HCI with both the spatial mean and coefficient of variance (CV) to assess whether thermal habitat area relates to changes in abundance (or diversity) and heterogeneity of the indicator. Total krill is dominated by two species, *Euphausia pacifica* and *Thysanoessa spinifera*, and northern anchovy consists of both young-of-the-year (YOY) and adult catches. The forage diversity (Shannon-Weaver) index includes coastal and mesopelagic fish and squid, totaling 49 taxa (Santora et al. 2017). Total diversity is calculated from the CPUE of all 111 taxa consistently caught in RREAS mid-water trawls, including YOY rockfish and other groundfish, the forage species described above, and several other well enumerated taxa. All data are available at https://oceanview.pfeg.noaa.gov/erddap/tabledap/.

Wind-driven upwelling is hypothesized to have a cumulative effect on regional ecosystem productivity and structure in EBUEs (Bograd et al. 2009). Historically, the Cumulative Upwelling Index (CUI; Schwing et al. 2000; Bograd et al. 2009) has been used as an index of this productivity, with winter values being better aligned with spring productivity due to 'pre-conditioning' effects on the ecosystems (Schroeder et al. 2013). Here, we test if productivity associated with the distribution and aggregation of fish and krill are more associated with traditional indices or the HCI based on the cumulative effect of the expansion or contraction of thermal habitat along the coast. We test this by constructing 4 cumulative time series, based on daily BEUTI, CUTI, sea level and the HCI. The BEUTI and CUTI time series are created by latitudinally averaging all daily time series between 36 and 40°N to obtain a single time series. The sea level time series is from a tide station at San Francisco, CA (previously discussed at stat of this section). Then the cumulative sum from January through February is computed for each year, resulting in a final annual cumulative BEUTI (cBEUTI), CUTI (cCUTI), and Sea Level (cSea Level) time series. The cumulative time series are correlated against the RREAS time series using Spearman's rank correlations and significance was determined at $p < 0.05$.

3. Results and discussion

3.1. Regional and seasonal habitat compression indices

Regionally and monthly resolved temperature thresholds are necessary in the CCLME due to the large meridional temperature gradients and spatially-varying seasonal cycle in surface temperature (Fig. 1b, 2a, Supplemental Fig. S.2). The difference between northern and southern extremes can vary by 6 °C in winter and 4 °C in summer. At the scale of the CCLME, temperature gradients are predominately meridional in the winter and spring, with cooler temperatures to the north, although there

is a strong zonal temperature gradient in the Southern California Bight. Upwelling during the summer and fall results in zonal gradients of cooler water nearshore, with the largest gradients in Regions 2 and 3 (Fig. 1, Supplemental Fig. S.2). In Region 4, temperatures north Pt. Conception (~34.5°N) are consistently cooler by over 1 °C than temperatures in the Southern California Bight. When zonal SST gradients are weak, HCI values may be less informative for monitoring a habitat compression impact. However, rapid changes (over a month) during an ocean warm event (heatwave or El Niño) may alter the anisotropy of habitat compression and create different warm and cool spatial patterns within and among regions. Regardless, the area of cool thermal habitat can vary spatially, extending in both meridional and zonal gradients, which reinforces the necessity to evaluate the HCI as a time series and as a mapped product.

Monthly climatologies of spatially averaged (from shore out to 75 km) T_{2m} have the expected seasonal cycle of cooler temperatures in winter and spring and warmer values during summer and fall (Fig. 2a). Over the four regions, December through May climatological values are the most consistent, with values generally within 1 °C of each other. The largest increase in temperatures occurs during June to September, with up to 1.5 °C between months (seen in Regions 1 and 4). A similar pattern occurs over September to October but for decreasing temperatures. Regions 1 and 4 have the greatest differences between the coolest and warmest months (~5 °C), while the difference is only around 3 °C for Regions 2 and 3. The ranges of temperature differences between months and over regions highlights the necessity for monthly and regionally

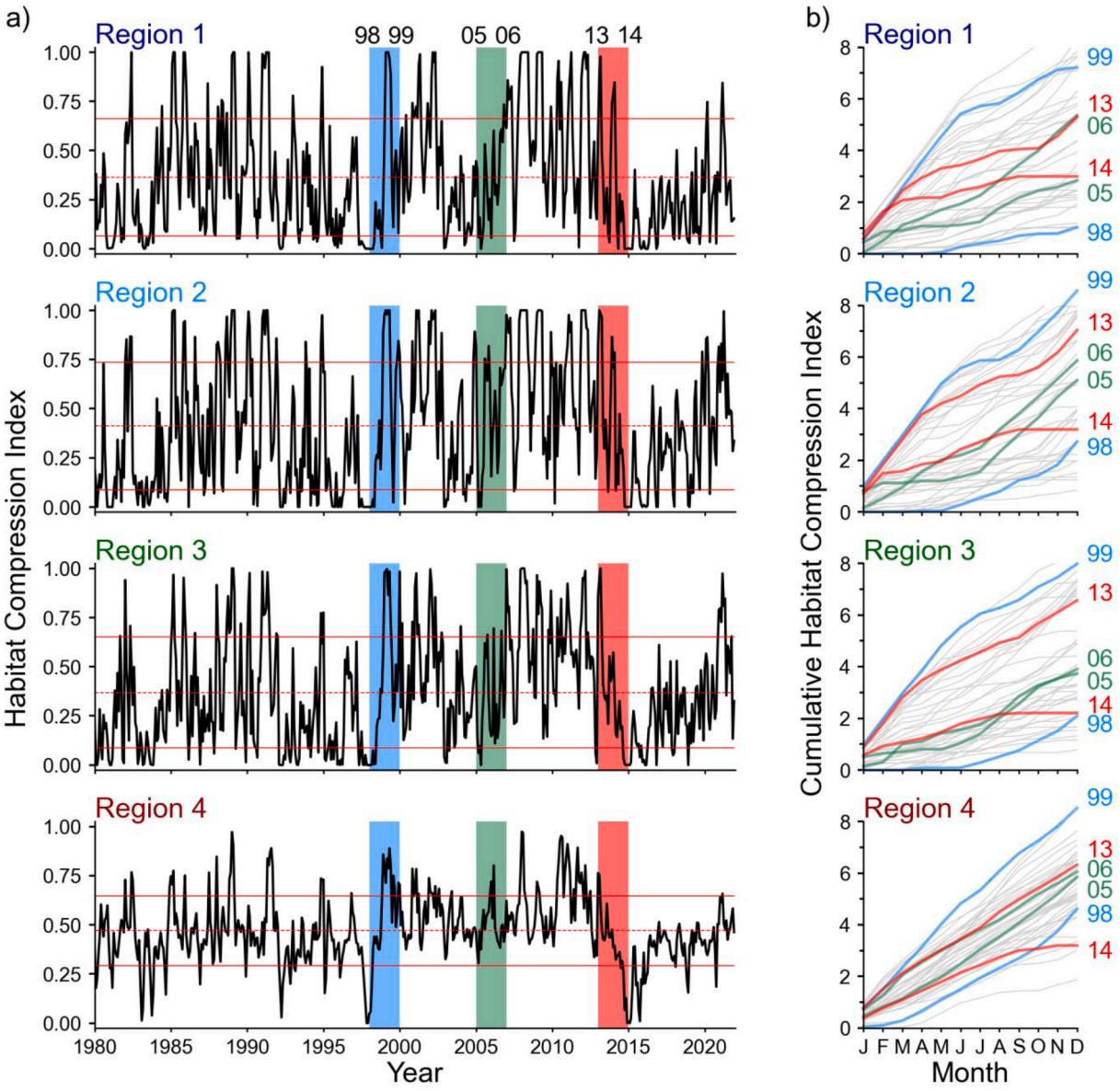

Fig. 3. Long-term regional variability of habitat compression indices: (a) Monthly Habitat Compression Index (HCI) time series shown for the four regions in the CCLME. The HCI denotes the amount of area covered by temperatures below a monthly temperature threshold, with '0' indicating no area and '1' total coverage. Dashed line is the mean and solid lines are ±1 standard deviations. Three separate two-year intervals (1998–99, 2005–06, and 2013–14) are marked to show HCI transitions during recent years of significant ecological impacts. These years were selected for illustration purposes to highlight marked change during a strong El Niño to La Niña (98–99), a period of delayed upwelling (05–06) and a period of record upwelling before the start of the large marine heatwave (13–14). (b) Cumulative Habitat Compression Index (cHCI) for the four regions. Each year (1980–2020) has a unique cumulative curve and is constructed by the cumulative sum over the twelve months of the year. The cumulative index approach allows for monitoring the rate of change of cool thermal habitat and provides information on changes from winter to spring (preconditioning effects on ecosystem). The maximum value of a monthly HCI is 1, with the maximum value of the cumulative curve at December being 12. The six years highlighted in plot (a) are drawn with the highlight color and labeled, while all other years are colored grey.

resolved temperature thresholds. To highlight this, an example HCI calculation is considered over June 2014 for Region 3 (Fig. 2b). The Region 3 temperature threshold for June is 12.5 °C and temperatures falling below this threshold cover 29,177 km^2 out of a total 89,418 km^2, resulting in an HCI value of 0.33. Region 4 has a June temperature threshold of 16.5 °C and if this is applied to Region 3 for June 2014 then the resulting HCI will be 1 since all temperature values in the region fall below the threshold.

The HCI for the northern two regions have larger standard deviations (0.30 for Region 1 and 0.32 for Region 2), while the southern region has the smallest (0.18), consistent with the weaker seasonality in upwelling and temperature regimes from north to south (Fig. 3). The HCI long-term mean in Region 4 is 0.47 and is the closest to 0.5, while the other regions all have means below 0.41. The HCI among regions are highly correlated with the highest correlations occurring between adjacent regions, and with winter and spring time series having higher correlations than summer and fall (Supplemental Fig. S.3). These results are consistent with Mueter et al. (2002), who found that spatial correlations for both NE Pacific upwelling and sea surface temperatures were strongest during winter months and weakest during summer months. The HCI calculated from NOAA's optimally interpolated SST yield consistent time series with ROMS model output (Spearman's ρ values above 0.9, with the lowest correlation of 0.84 during the summer in Region 3; Supplemental Fig. S.4). Therefore, a HCI can be easily estimated from other gridded SST data products and applied in other EBUSs to benefit ecological investigations.

3.2. Habitat compression and mixed layer depth

Unique HCIs are constructed for depths of 2, 10, 20, and 40 m, as these depths represent average seasonal extent of the mixed layer depth (MLD) within the CCLME (Fig. 4). The MLDs of the near-coastal CCLME are deeper in winter and spring and shoal during summer and fall (Fielder 1988, Fielder et al. 2013). In general, the MLDs estimated by Fielder (1988) are between 20 and 40 m during winter and spring, and between 14 and 20 m during summer and fall. Time series of HCI by depth have the most similarity between the 2 and 10 m time series, with the correlations weakening for the 20 and 40 m time series (Supplemental Figs. S.5, S.6). Winter and spring time series have high correlations over all depths to 40 m, while summer and fall have the highest correlations between the 10 and 20 m time series. The 40 m time series have the lowest correlations with the 2 m time series in summer and fall (ρ ranges 0.6 to 0.8), seasons where the MLDs are above the 40 m level. The HCI at 2 m has the largest difference compared to other depths during the last seven years (Supplemental Figs. S.5, S.6), a period impacted by a prolonged MHW (Jacox et al. 2018b). During this period, the HCI at 2 m during summer and fall is smaller than the HCI based on temperatures at depths of 10 m, 20 m, and 40 m. However, it should be noted that the MHWs occurred during the running period of the NRT ROMS and the divergent HCIs over the depths could be associated with inconsistencies between the two ROMS models. Nevertheless, the comparison of compression indices over several depths up to the average MLD suggests the HCI is consistent over space and time, and across the depth dimension (i.e., not just the surface). This is important because species distribution models often use satellite sea surface temperature even though those species are likely to respond to changes across the MLD range and deeper.

3.3. Habitat compression as an indicator of climate variability

For over 40 years, the regional HCI time series display marked coherence, with consistent inter-annual variability and response to

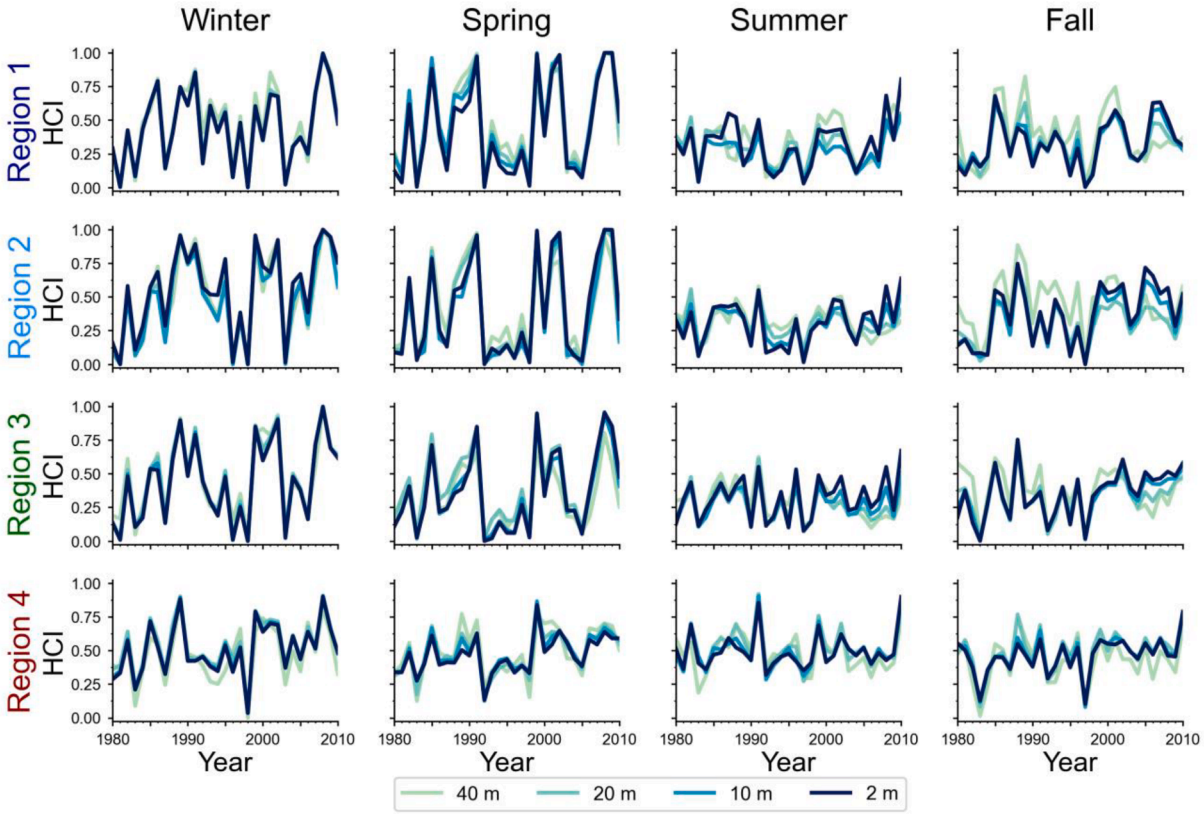

Fig. 4. Habitat compression index comparison by region (figure rows) over the mixed layer depth, with the comparisons done with four depths down to 40 m. The time period is from 1980 to 2010 covering the climatological time period of the ROMS historical model. The comparisons are done by season (columns) to best capture the seasonality of the changing mixed layer across the California Current as the MLD shifts to shallower depths during the summer from the deepest depths during the winter. For each depth a unique HCI was constructed using the same temperature threshold monthly selection methodology as for the surface (2 m) HCI.

climate events such as several tropical ENSO events and prolonged MHWs (Fig. 3). Here we highlight several prominent climate events that occurred in the CCLME during the study period along with the response of the HCI. The monthly progression of HCI values have the greatest shifts during ENSO transition periods with values shifting from 0 (a tropical El Niño year) to 1 (a tropical La Niña year) over a two-year period (see shaded area over 1998–99; Fig. 3a). El Niño and La Niña produce extensive ecological impacts in the CCLME due to deepening and shoaling of the nutricline (Bograd and Lynn 2001) and upper ocean warming and cooling, respectively (McClatchie et al 2016). Other two-year periods of unusual ecosystem dynamics in the CCLME were 2005–06 and 2013–14 (shaded regions; Fig. 3a). The 2005–06 HCI values mostly fall within one standard deviation of the mean, with very few months (Region 3 October 2005 and March and September 2006) above one standard deviation. Starting in late 2004 and early 2005 all regions experienced HCI values more than one standard deviation below their long-term mean. There were 1–3 month delays in the onset of seasonal upwelling during 2005 and 2006 that resulted in major population declines of many forage species, particularly YOY groundfish, market squid and krill (Ralston et al. 2015). These in turn contributed to reproductive failures for many seabirds, unusual marine mammal distributions, and later economic fishery disaster declarations associated with poor adult salmon run-sizes returns (Sydeman et al. 2006, Weise et al. 2006, Lindley et al. 2009). Over 2013–14 the HCI transitioned from high to low cool-water habitat area due to the influences of an expanding MHW (Jacox et al. 2018b, Santora et al. 2020). The HCI values progressed from over one standard deviation at the start of 2013, a year of very strong upwelling, and finally reached values near 0 at the end of 2014 when the MHW had major impacts on the CCLME (Di Lorenzo and Mantua 2016).

As a measure of thermal habitat that is relevant for monitoring ecosystem state and fisheries, the annual evolution of the HCI can inform dynamic ocean management in the CCLME. Cumulative HCI curves were constructed for all years and regions, with the same two-year periods of 1998–99, 2005–06, and 2013–14 to highlight the yearly progression of habitat compression and expansion (Fig. 3b). The cHCI over 1998 spanned a transition period from a strong tropical El Niño to La Niña, had a low amount of cool-water habitat during winter 1998 and the 3 northern regions had HCI values of 0 through the winter (January-March in Region 3) and early spring (January-April in Region 1 and 2). HCI values increased after spring 1998, tracking the transition from El Niño to La Niña conditions (Chavez et al. 2002; Bograd and Lynn, 2001), and winter and spring 1999 HCI values were near 1 resulting in 1999 having one of the highest December cHCI values. This is consistent with observations of unusually strong coastal upwelling and low sea surface temperatures throughout most of the CCLME during the spring and summer of 1999 (Schwing et al. 2000). Both 2005 and 2006 have similar annual cHCI values and are near the median range across all years. However, winter and spring 2005 and 2006 both started off with very small HCI values, then rapidly transitioned to larger HCI values during summer and fall. During 2013, large values of the cHCI (for each region) over January to March were similar to 1999, but low HCI values during summer resulted in final December cHCI values smaller than in 1999. January and February 2014 had high HCI values, especially in Regions 1 and 2, but the rest of the year had very low HCI values, resulting in 2014 having a similar cHCI December value as 1998. The development of the

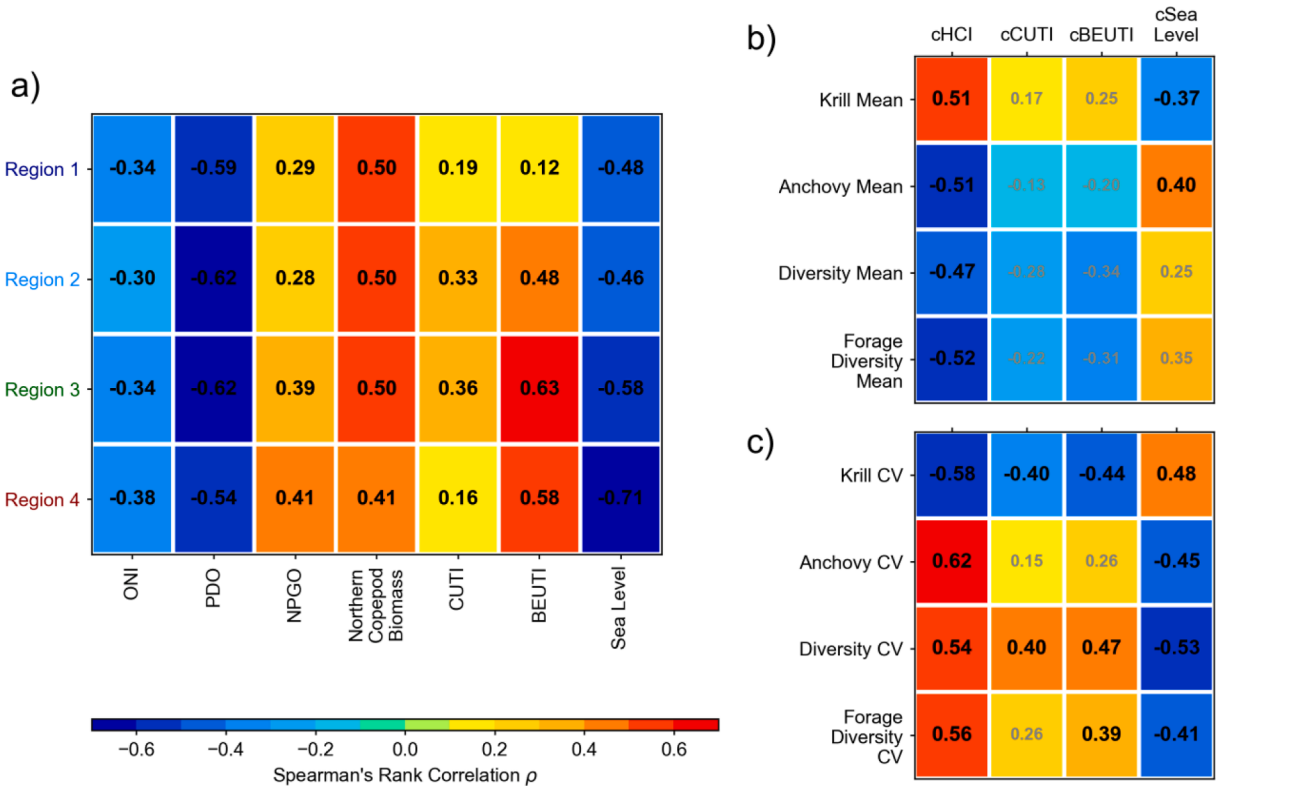

Fig. 5. Comparison of the Habitat Compression Indices to basin-scale and regional indicators of oceanographic variability in the CCLME and to the abundance, distribution and diversity of key forage species in the central CCLME. (a) Correlations between regional HCIs and monthly physical basin-scale indicators (ONI, PDO, NPGO), an indicator of subarctic transport (northern copepod biomass anomaly), spatial average of upwelling (CUTI and BEUTI) in each HCI region, and Sea Level measure by tidal gauges in the four HCI regions. (b) Correlations between annual spatial mean biological time series and January to February cumulative values of the regional indicators: cHCI, cCUTI, cBEUTI, and cSea Level. (c) Correlations between annual coefficient of variance (CV) biological time series and the same cumulative time series used in table (b). Biological data are from an ecosystem survey (RREAS) that samples during late April through June at stations located in Region 3. Correlations are Spearman's rank correlations. All correlations are below $p < 0.01$ for plot (a) and $p < 0.05$ for plots (b) and (c), except those labeled with grey text.

marine heatwave (the "Blob") during 2013 and 2014 (Bond et al 2014) resulted in low HCI due to the intrusion of warm off shore waters onto the shelf causing fluctuations and distribution shifts of humpback whales' prey (Santora et al. 2020) and consequent management challenges for the economically important Dungeness crab fishery (Samhouri et al 2021).

The 4 regional HCIs were compared to three basin-scale indices (PDO Index, ONI, and NPGO Index), and the PDO Index had the highest correlations (Fig. 5). The PDO Index correlations were negative, implying that a negative-cool phase of the PDO is related to a larger HCI value. ONI and HCI correlations were around −0.3, capturing the tendency for smaller HCI values during an El Niño event (Fiedler and Mantua 2017). The NPGO Index had a positive correlation with the HCIs and high habitat (large HCI values) are associated with an increased equatorward flow within the CCLME that is evident during positive NPGO phases (Di Lorenzo et al. 2013). Interestingly, the southern Region 4 HCI had the strongest relationship with the NPGO, as positive NPGO values are associated with a deeper upwelling cell in the southern CCLME resulting in more vertical mixing of cooler, deeper waters into the surface layer (Di Lorenzo et al. 2008). Sea level time series have a negative correlation with the HCIs, and CUTI and BEUTI have a positive relationship. Low sea levels and strong upwelling occur during an expansion of cool-water habitats, and vice-versa. Sea level in Region 4 has the highest correlation with the HCI of all of the basin and regional physical indices with a Spearman's ρ of −0.71 ($p < 0.01$). The correlations with BEUTI are higher than CUTI, which is expected due to BEUTI being more closely related to temperatures within the mixed layer (Jacox et al. 2018a).

3.4. Biological impacts of varying habitat compression

The HCI has been used by management as a spatial indicator for monitoring ecosystem shifts and species interactions (Santora et al. 2021). Here we compare the HCI with several biological indices that are included in annual reports on ecosystem status and trends to provide ecosystem context to the Pacific Fisheries Management Council (PFMC; Harvey et al., 2020). The ecological evaluation of the HCI should be framed as a hypothesis in order to accumulate additional support for monitoring ecosystem shifts in coastal upwelling systems and developing additional process-based studies involving species assemblage and indicator species analyses. Here we highlight several ecological indices to assess the hypothesis that cool water habitat compression impacts pelagic biodiversity and ecosystem function in the CCLME.

The northern copepod biomass anomaly time series is related to the PDO Index and salmon productivity (Peterson and Schwing 2003, Peterson et al. 2014), and has a positive correlation with the HCI over the four regions (Fig. 5a). The cool phase of the PDO corresponds with higher HCI (expanded cool habitat) and increased northern copepod species richness. Biological time series from the RREAS trawl consist of both spatial mean and coefficient of variance (CV; Supplemental Figs. S.7, S.8, S.9, S.10). The CV is an indicator of variance among biological survey locations within regions, with a lower CV occurring during years of uniform (less heterogeneity) spatial abundances (or diversity). The mean and CV time series are correlated against time series representing the cumulative effects of thermal habitat size (cHCI), upwelling intensity variables (cCUTI and cBEUTI) and sea level height (cSL).

The cHCI time series analysis had significant correlations against all ecological time series and the magnitude of the correlations were higher than traditional upwelling indices and sea level (Fig. 5b). The higher cHCI correlations suggest that cumulative (over January to February) thermal habitat is a better early indicator of abundances, diversity, and heterogeneity for the example species than cumulative upwelling over the same time period. Since cHCI has a better fit, the remaining discussion of the results will focus on the correlations with cHCI.

Here we show an example of how the cumulative cool thermal habitat area over January to February relates to epipelagic forage species abundances, diversity and spatial variance within central California (Fig. 5b-c). Northern anchovy relative abundance has a negative correlation with cHCI ($\rho = -0.51$, $p < 0.01$), with higher abundance sampled during years with less cool thermal habitat. Correlations between the cHCI and krill relative abundance and krill spatial variance (CV) are negative, indicating krill are more abundant and spatially less variable during years of higher HCI values (Santora et al. 2014, 2021b). Total diversity and forage species diversity time series are negatively correlated with the cHCI, indicating greater pelagic biodiversity during periods of warmer ocean conditions and high habitat compression (Santora et al. 2017). However, both diversity CV time series are positively correlated with cHCI ($\rho = -0.54$, $p < 0.01$ and $\rho = -0.56$, $p < 0.01$; respectively), suggesting increased heterogeneity of diversity patterns occurs when there is lower habitat compression (less cool thermal habitat). We recommend comparing the HCI with other ecological indicators as a process to help refine regional mechanisms relating thermal habitat area to ecosystem shifts.

3.5. Implications for ecosystem monitoring and management

We have shown that the HCI is a meaningful and informative ecosystem indicator that describes changes in thermal habitat area translating to variability of ecosystem function. We recommend that other temperate upwelling ecosystems investigate compression indices to measure thermal habitat area relative to ecosystem conditions. Using ocean model or observation-based gridded SST data, the HCI concept is easily extendable to other ecosystems where it may be desirable to monitor thermal habitat variability to inform fisheries and ecosystem assessments. Specifically, in ecosystems where krill and coastal pelagic species are dominant pathways of trophic transfer, an HCI could be used for testing predictions on how ecosystem function may change due to natural and anthropogenic climate change and variability. The HCI directly indexes habitat used by cool-water species that can lead to greater interaction with human activities.

Large marine heatwaves impact coastal upwelling ecosystems through compression of cool thermal habitat closer to the shore (Santora et al. 2020). Therefore, the HCI approach may be useful for tracking the spatial extent of cool water during marine heatwaves. Between 2013 and 2021 the Northeast Pacific Ocean experienced episodes of unusual warm sea surface temperatures related to multiple marine heatwaves (Bond et al., 2015; Amaya et al. 2020) and a large El Niño event that impacted the CCLME during fall of 2015 (Jacox et al. 2016) and smaller El Niño events in 2018 and 2019 (Thompson et al. 2019). MHWs can cause disruptions in CCLME function ranging from persistent harmful algal blooms, shifts in copepod community composition and coastal pelagic species distribution, and socio-ecological impacts involving fisheries and increased human-wildlife interactions such as whale entanglements (Cavole et al. 2016; Santora et al. 2020). However, not all was bad for CCLME marine life during the 2014–16 MHW as this period coincided with record high abundance of young-of-year groundfish (Santora et al. 2017; Schroeder et al. 2019; Field et al. 2021) and potentially influenced substantial recruitment and population growth of northern anchovy (Santora et al. 2021). Di Lorenzo and Mantua (2016) concluded from a modeling study that the variance in ocean basin-scale patterns associated with marine heatwaves might increase significantly under future climate scenarios. We show that within temperate upwelling systems, the HCI can track changes in thermal habitat area, either due to MHW or shifts in contributions from subarctic or subtropical source waters that alter ocean conditions and ecosystem structure (Schroeder et al. 2019; Santora et al. 2021).

We previously demonstrated the importance of the HCI for understanding and mitigating whale entanglements with commercial Dungeness crab (*Cancer magister*) fishing gear that occurred during a prolonged MHW (Santora et al. 2020). This fishery is often the most economically valuable commercial fishery on the U.S. West Coast. The ecosystem synthesis involving the HCI was an integral part in the

development of the whale entanglement Risk Assessment and Mitigation Program (RAMP). The index was further refined as a management and communication tool to support a consortium of stakeholders, ranging from fishers, conservation organizations, scientists and fishery managers that are dedicated to providing solutions to prevent whale entanglements and detrimental impacts to whale populations and coastal fishing communities (including people engaged in fishing, processing and other related jobs). The HCI helps to inform management decisions regarding the opening and closure of the fishery by providing near real time information on how the ecosystem is changing, critical given the complex nature of interactions between the fishery, the ecosystem and the protected species (whales) that are disproportionately impacted during adverse ocean conditions. As part of this study to extend access to ecosystem information, we developed a website that serves the HCI, along with other ecosystem information for fishery managers to make real time decisions to benefit fishery management on the U.S. West Coast (https://www.integratedecosystemassessment.noaa.gov/regions/california-current/ecosystem-context-reducing-west-coast-whale-entanglements). As other fixed gear fisheries can lead to whale entanglements, and impacts to fishing opportunities in the Dungeness crab fishery also have implications to federally managed groundfish and salmon (among other) fisheries, the HCI is also included in the NOAA California Current Integrated Ecosystem Assessment's annual ecosystem status report provided to the Pacific Fishery Management Council, highlighting its utility to management.

The phenology of regional SST and associated thresholds described in this study provide informative reference points for the ecosystem monitoring in the CCLME (Figs. 1-2). Species distribution models often indicate that SST is an important predictor of suitable habitat and for informing dynamic ocean management and monitoring potential range shifts of protected species and fishery resources (Brodie et al. 2018). Most marine species distribution models have strong seasonal cycles that are due to dependence on SST (Becker et al. 2016; Brodie et al. 2018). For example, predictions of suitable anchovy habitat, albacore (*Thunnus alalunga*) habitat expansion and occurrence of blue whales (*Balaenoptera musculus*), all largely depend on the seasonal variability of SST (Muhling et al. 2020; Abrahms et al. 2019) and often display pronounced south to north progression of predicted suitable habitat within the CCLME. However, researchers have not identified regional or basin-wide scales of variability associated with the phenology of SST to assess why species distributions change the way they do in response to ocean climate forcing. Correlative models used to make predictions of habitat suitability from SST may overemphasize particular temperature thresholds particularly if species show non-stationary relationships with environmental predictors. Useful ecosystem indicators can be used in lieu of multiple SDMs which be laborious and data-hungry to fit.

Beyond the thermal habitat compression index, the SST reference points we quantified provide a basis for understanding why and how species habitat suitability models are expected to have such strong seasonal variability throughout the CCLME. If species response to SST shows a particular sensitivity or threshold change, then the reference points we identified will be useful in developing scenarios on how species may change in the future. For example, coastal pelagic species, such as anchovy, sardine and market squid, have specific thermal ranges that are conducive to spawning, which is also an aggregative response to available thermal habitat (Reiss et al., 2008, Zwolinski et al. 2011, Zeidberg et al., 2011). This baseline phenology of SST information alone is useful for understanding species thermal habitat associations and for developing climate vulnerability assessments and mitigating tradeoffs regarding management of protected species and fished resources. We recommend comparison of output from species habitat suitability and density distribution models with regional HCIs to refine understanding of SST thresholds and ecological structure of coastal upwelling systems.

The HCI provides measurable and meaningful context for assessment of ecological consequences resulting from thermal habitat compression within coastal upwelling ecosystems. The unique information of the HCI pertaining to thermal habitat area allows us to examine the extent to which key biological interactions and processes are compressed in the coastal zone. Our ongoing efforts to inform management of the Dungeness crab fishery with respect to entanglement risk to large whales in response to habitat compression and other factors provides an example of how this information can be used to help inform management decisions. It should be kept in mind that the extension of the HCI to assessment of ecosystem function should be cast as hypothesis development to ensure that evidence can be accumulated for specific research questions (Santora et al. 2021). Beyond mitigating whale entanglement risk, there are other compression impacts on managed and protected species that are associated with compressed cold-water habitat (Wells et al. 2017; Cimino et al. 2022). Applications could include assessment of impacts of increased overlap between mobile predators, prey, and fisheries that favor cold-water habitats, increasing the intensity and frequency of interactions in ways that might alter competition, predation rates and recruitment rates, changes in natural mortality rates or vulnerability to fisheries. For example, with high compression of cold-water habitat, salmon fisheries may operate on what effectively becomes a smaller ocean for salmon (where West Coast Chinook salmon typically feed and are caught in areas with summertime SSTs ~ 10–14 °C), potentially resulting in abnormally high catches for a given stock size. Salmon fishery management decisions rely on estimated contact rates in sport and commercial fisheries for different age-classes and stocks (targeted and protected) in mixed-stock fisheries. Such fishery decisions might benefit by considering changes in thermal habitat extent (Shelton et al. 2021). Regional reduction of thermal habitat may lead to reduced carrying capacity for species dependent on pelagic cold-water habitat, including the seasonal migrants (seabirds, turtles, marine mammals, and highly migratory species). Ecosystem shifts associated with offshore pelagic organisms moving shoreward may result in increased presence of tropical/sub-tropical species and their increased availability to fishers, such as Bluefin tuna (*Thunnus thynnus*), which show a link between changing distribution and SST (Block et al. 2011; Carroll et al. 2021). Such shifts can create new human-wildlife conflict affecting fisheries, protected species, and fishing communities (Santora et al. 2020). Finally, we recommend that ocean climate modelers that develop future projections examine changes in habitat compression, especially under different climate scenarios.

Declaration of Competing Interest

The authors declare that they have no known competing financial interests or personal relationships that could have appeared to influence the work reported in this paper.

Data availability

Data will be made available on request.

Acknowledgements

We thank the NOAA West Coast Regional Office, Protected Species Division, California Current Integrated Ecosystem Assessment (CCIEA) team, Lynn De Witt and Greg Williams. Support was provided by the U.S. Marine Biodiversity Observation Network (MBON), jointly funded by NOAA, NASA and the National Oceanographic Partnership Program (80NSSC20M0001).

Appendix A. Supplementary data

Supplementary data to this article can be found online at https://doi.org/10.1016/j.ecolind.2022.109520.

References

Amaya, D.J., Miller, A.J., Xie, S., et al., 2020. Physical drivers of the summer 2019 North Pacific marine heatwave. Nat. Commun. 11, 1903. https://doi.org/10.1038/s41467-020-15820-w.

Bakun, A., Black, B.A., Bograd, S.J., García-Reyes, M., Miller, A.J., Rykaczewski, R.R., Sydeman, W.J., 2015. Anticipated effects of climate change on coastal upwelling ecosystems. Current Climate Change Reports 1, 85–93.

Becker, E.A., Forney, K.A., Fiedler, P.C., Barlow, J., Chivers, S.J., Edwards, C.A., Moore, A.M., Redfern, J.V., 2016. Moving towards dynamic ocean management: how well do modeled ocean products predict species distributions? Remote Sensing 8 (2), 149.

Block, B.A., Jonsen, I.D., Jorgensen, S.J., Winship, A.J., Shaffer, S.A., Bograd, S.J., Hazen, E.L., Foley, D.G., Breed, G.A., Harrison, A.L., Ganong, J.E., 2011. Tracking apex marine predator movements in a dynamic ocean. Nature 475 (7354), 86–90.

Bograd, S.J., Lynn, R.J., 2001. Physical-biological coupling in the California Current during the 1997–99 El Niño-La Niña cycle. Geophys. Res. Lett. 28 (2), 275–278.

Bograd, S.J., Schroeder, I., Sarkar, N., Qiu, X., Sydeman, W.J., Schwing, F.B., 2009. Phenology of coastal upwelling in the California Current. Geophys. Res. Lett. 36 (1).

Bond, N.A., Cronin, M.F., Freeland, H., Mantua, N., 2015. Causes and impacts of the 2014 warm anomaly in the NE Pacific. Geophys. Res. Lett. 42, 3414–3420. https://doi.org/10.1002/2015GL063306.

Brodie, S., Jacox, M.G., Bograd, S.J., Welch, H., Dewar, H., Scales, K.L., Hazen, E.L., 2018. Integrating dynamic subsurface habitat metrics into species distribution models. Front. Mar. Sci. 5, 219. https://doi.org/10.3389/fmars.2018.00219.

Carroll, G., Brodie, S., Whitlock, R., Ganong, J., Bograd, S.J., Hazen, E., Block, B.A., 2021. Flexible use of a dynamic energy landscape buffers a marine predator against extreme climate variability. Proc. R. Soc. B 288, 20210671. https://doi.org/10.1098/rspb.2021.0671.

Cavole, L.M., Demko, A.M., Diner, R.E., Giddings, A., Koester, I., Pagniello, C.M., Paulsen, M.L., Ramirez-Valdez, A., Schwenck, S.M., Yen, N.K., Zill, M.E., 2016. Biological impacts of the 2013–2015 warm-water anomaly in the Northeast Pacific: winners, losers, and the future. Oceanography 29 (2), 273–285.

Chavez, F.P., Messié, M., 2009. A comparison of eastern boundary upwelling ecosystems. Prog. Oceanogr. 83 (1–4), 80–96.

Chavez, F.P., Pennington, J.T., Castro, C.G., Ryan, J.P., Michisaki, R.P., Schlining, B., Walz, P., Buck, K.R., McFadyen, A., Collins, C.A., 2002. Biological and chemical consequences of the 1997–1998 El Niño in central California waters. Prog. Oceanogr. 54 (1–4), 205–232.

Chavez, F.P., Ryan, J., Lluch-Cota, S.E., Ñiquen, M., 2003. From anchovies to sardines and back: multidecadal change in the Pacific Ocean. Science 299 (5604), 217–221.

Checkley, D.B., Alheit, J., Oozeki, Y., Roy, C., 2009. Climate Change and Small Pelagic Fish. Cambridge University Press, Cambridge.

Cimino, M.A., Santora, J.A., Schroeder, I., Sydeman, W., Jacox, M.G., Hazen, E.L., Bograd, S.J., 2020. Essential krill species habitat resolved by seasonal upwelling and ocean circulation models within the large marine ecosystem of the California Current System. Ecography 43, 1536–1549. https://doi.org/10.1111/ecog.05204.

Cimino, M.A., Shaffer, S.A., Welch, H., Santora, J.A., Warzybok, P., Jahncke, J., Schroeder, I., Hazen, E.L., Bograd, S.J., 2022. Western gull foraging behavior as an ecosystem state indicator in Coastal California. Front. Mar. Sci. 8, 790559.

Di Lorenzo, E., Mantua, N., 2016. Multi-year persistence of the 2014/15 North Pacific marine heatwave. Nature Clim. Change 6, 1042–1047. https://doi.org/10.1038/nclimate3082.

Di Lorenzo, E., Schneider, N., Cobb, K.M., Franks, P.J.S., Chhak, K., Miller, A.J., McWilliams, J.C., Bograd, S.J., Arango, H., Curchitser, E., Powell, T.M., Riviere, P., 2008. North Pacific Gyre Oscillation links ocean climate and ecosystem change. Geophys. Res. Lett. 35 https://doi.org/10.1029/2007gl032838.

Di Lorenzo, E., Combes, V., Keister, J.E., Strub, P.T., Thomas, A.C., Franks, P.J., Ohman, M.D., Furtado, J.C., Bracco, A., Bograd, S.J., Peterson, W.T., 2013. Synthesis of Pacific Ocean climate and ecosystem dynamics. Oceanography 26 (4), 68–81.

Fiedler, P.C., Mantua, N.J., 2017. How are warm and cool years in the California Current related to ENSO? J. Geophys. Res. Oceans 122 (7), 5936–5951.

Fisher, J.L., Peterson, W.T., Rykaczewski, R.R., 2015. The impact of El Niño events on the pelagic food chain in the northern California Current. Global Change Biol. 21, 4401–4414.

Friedman, W.R., Santora, J.A., Schroeder, I.D., Huff, D.D., Brodeur, R.D., Field, J.C., Wells, B.K., 2018. Environmental and geographic relationships among salmon forage assemblages along the continental shelf of the California Current. Mar. Ecol. Prog. Ser. 596, 181–198.

Hickey, B.M., 1998. Coastal Oceanography of Western North America from the tip of Baja California to Vancouver Island. In: Brink, K.H., Robinson, A.R. (Eds.), The Sea, Volume 11. Wiley and Sons Inc, New York, NY, pp. 345–393.

Hickey, B.M., Banas, N.S., 2008. Why is the northern end of the California Current System so productive? Oceanography 21 (4), 90–107.

Holland, D.S., Leonard, J., 2020. Is a delay a disaster? economic impacts of the delay of the California dungeness crab fishery due to a harmful algal bloom. Harmful Algae 98, 101904.

Huang, B., C. Liu, V. Banzon, E. Freeman, G. Graham, B. Hankins, T. Smith, H.-M. Zhang. Improvements of the daily optimum interpolation sea surface temperature (doisst) version 2.1. 2020. Journal of Climate, pages 1 – 47, doi: 10.1175/JCLI-D-20-0166.1.

Hubbs, C.L., 1948. Changes in the fish fauna of western North America correlated with changes in ocean temperature. J. Mar. Res. 7 (3), 459–482.

Huyer, A 1983. Coastal upwelling in the California current system. Progress in Oceanography, 12: 259-284, ISSN 0079-6611, doi: 10.1016/0079-6611(83)90010-1.

Jacox, M.G., Edwards, C.A., Hazen, E.L., Bograd, S.J., 2018. Coastal upwelling revisited: Ekman, Bakun, and improved upwelling indices for the US West Coast. J. Geophys. Res.-Oceans 123, 7332–7350.

Jacox, M.G., Alexander, M.A., Mantua, N.J., Scott, J.D., Hervieux, G., Webb, R.S., Werner, F.E. 2018b. Multiyear extreme ocean temperatures with impacts on living marine resources off the US west coast during 2016. [in "Explaining Extreme Events of 2016 from a Climate Perspective"]. Bull. Amer. Meteor. Soc., 99 (1), S27-S33, doi: 10.1175/BAMS-D-17-0119.1.

Jacox, M., Hazen, E., Bograd, S., 2016. Optimal environmental conditions and anomalous ecosystem responses: constraining bottom-up controls of phytoplankton biomass in the California Current System. Sci Rep 6, 27612. https://doi.org/10.1038/srep27612.

King, J.R., Agostini, V.N., Harvey, C.J., McFarlane, G.A., Foreman, M.G., Overland, J.E., Di Lorenzo, E., Bond, N.A., Aydin, K.Y., 2011. Climate forcing and the California Current ecosystem. ICES J. Mar. Sci. 68 (6), 1199–1216.

Lindley, S.T., Grimes, C.B., Mohr, M.S., Peterson, W., Stein, J., Anderson, J.T., Botsford, L.W., Bottom, D.L., Busack, C.A., Collier, T.K., Ferguson, J., Garza, J.C., Grover, A.M., Hankin, D.G., Kope, R.G., Lawson, P.W., Low, A., MacFarlane, R.B., Moore, K., Palmer-Zwahlen, M., Schwing, F.B., Smith, J., Tracy, C., Webb, R., Wells, B.K., Williams, T.H., 2009. What caused the Sacramento River fall Chinook stock collapse? NOAA Tech Memo. NOAA-TM-NMFS-SWFSC-447.

Mantua, N.J., Hare, S.R., Zhang, Y., Wallace, J.M., Francis, R.C., 1997. A Pacific interdecadal climate oscillation with impacts on salmon production. Bull. Am. Meteorol. Soc. 78, 1069–1079.

McClatchie, S. et al., 2016. State of the California Current 2015–16: comparisons with the 1997–98 El Niño. CalCOFI Rep., 57.

Moore, A.M., Arango, H.G., Broquet, G., Edwards, C., Veneziani, M., Powell, B., Foley, D., Doyle, J.D., Costa, D., Robinson, P., 2011. The Regional Ocean Modeling System (ROMS) 4-dimensional variational data assimilation systems Part II - Performance and application to the California Current System. Prog. Oceanogr. 91 (1), 50–73. https://doi.org/10.1016/j.pocean.2011.05.003.

Mueter, F.J., Ware, D.M., Peterman, R.M., 2002. Spatial correlation patterns in coastal environmental variables and survival rates of salmon in the north-east Pacific Ocean. Fish. Oceanogr. 11 (4), 205–218.

Neveu, E., Moore, A.M., Edwards, C.A., Fiechter, J., Drake, P., Crawford, W.J., Jacox, M. G., Nuss, E., 2016. An historical analysis of the California Current circulation using ROMS 4D-Var: System configuration and diagnostics. Ocean Modeling 99, 133–151. https://doi.org/10.1016/j.ocemod.2015.11.012.

Parrish, R.H., Nelson, C.S., Bakun, A., 1981. Transport mechanisms and reproductive success of fishes in the California Current. Biol. Oceanography 1 (2), 175–203.

Peterson, W.T., Miller, C.B., 1975. Year-to-year variations in the planktology of the Oregon upwelling zone. Fish. Bull. U.S. 73, 642–653.

Peterson, W.T., Fisher, J.L., Peterson, J.O., Morgan, C.A., Burke, B.J., Fresh, K.L., 2014. Applied fisheries oceanography: Ecosystem indicators of ocean conditions inform fisheries management in the California Current. Oceanography 27 (4), 80–89.

Peterson, W.T., Schwing, F.B., 2003. A new climate regime in northeast Pacific ecosystems. Geophys. Res. Lett. 30 (17).

Ralston, S., Field, J.C., Sakuma, K.M., 2015. Long-term variation in a central California pelagic forage assemblage. J. Mar. Syst. 146, 26–37.

Reiss, C.S., Checkley, D.M., Bograd, S.J., 2008. Remotely sensed spawning habitat of Pacific sardine (*Sardinops sagax*) and Northern anchovy (*Engraulis mordax*) within the California Current. Fish. Oceanogr. 17, 126–136. https://doi.org/10.1111/j.1365-2419.2008.00469.x.

Rice, J.C., Rochet, M.J., 2005. A framework for selecting a suite of indicators for fisheries management. ICES J. Mar. Sci. 62 (3), 516–527.

Ritzman, J., Brodbeck, A., Brostrom, S., McGrew, S., Dreyer, S., Klinger, T., Moore, S.K., 2018. Economic and sociocultural impacts of fisheries closures in two fishing-dependent communities following the massive 2015 US West Coast harmful algal bloom. Harmful Algae 80, 35–45.

Sakuma, K.M., Field, J.C., Mantua, N.J., Ralston, S., Marinovic, B.B., Carrion, C.N., 2016. Anomalous epipelagic micronekton assemblage patterns in the neritic waters of the California Current in spring 2015 during a period of extreme ocean conditions. CalCOFI Rep 57, 163–183.

Samhouri J.F., Feist B.E., Fisher M.C., Liu O., Woodman, S.M., Abrahms, B., Forney K.A., Hazen E.L., Lawson, D., Redfern J., and Saez L.E. 2021. Marine heatwave challenges solutions to human–wildlife conflict. Proc. R. Soc. B. 288 2021160720211607.

Santora, J.A., Hazen, E.L., Schroeder, I.D., Bograd, S.J., Sakuma, K.M., Field, J.C., 2017. Impacts of ocean-climate variability on biodiversity of pelagic forage species in an upwelling ecosystem. Mar. Ecol. Prog. Ser. 580, 205–220. https://doi.org/10.3354/meps12278.

Santora, J.A., Mantua, N.J., Schroeder, I.D., et al., 2020. Habitat compression and ecosystem shifts as potential links between marine heatwave and record whale entanglements. Nat Commun 11, 536. https://doi.org/10.1038/s41467-019-14215-w.

Santora, J.A., Schroeder, I.D., Bograd, S.J., Chavez, F.P., Cimino, M.A., Fiechter, J., Hazen, E.L., Kavanaugh, M.T., Messié, M., Miller, R.R., Sakuma, K.M., Sydeman, W. J., Wells, B.K., Field, J.C., 2021a. Pelagic biodiversity, ecosystem function, and services: An integrated observing and modeling approach. Oceanography 34 (2). https://doi.org/10.5670/oceanog.2021.212.

Santora, J.A., Rogers, T., Cimino, M.A., Sakuma, K.A., Hanson, K., Dick, E.J., Jahncke, J., Warzybok, P., Field, J.C., 2021b. Diverse integrated ecosystem approach overcomes pandemic-related fishery monitoring challenges. Nat. Commun. 6492 https://doi.org/10.1038/s41467-021-26484-5.

Schroeder, I.D., Black, B.A., Sydeman, W.J., Bograd, S.J., Hazen, E.L., Santora, J.A., Wells, B.K., 2013. The North Pacific High and wintertime pre-conditioning of California current productivity. Geophys. Res. Lett. 40 (3), 541–546.

Schroeder, I.D., Santora, J.A., Moore, A.M., Edwards, C.A., et al., 2014. Application of a data-assimilative regional ocean modeling system for assessing California Current System ocean conditions, krill, and juvenile rockfish interannual variability. Geophys. Res. Lett. 41, 5942–5950.

Schwing, F.B., Moore, C., Ralston, S., Sakuma, K.A., 2000. Record coastal upwelling in the California Current in 1999. Calif. Coop. Oceanic Fish. Invest. Rep. 41, 148–160.

Shelton, A.O., Sullaway, G.H., Ward, E.J., Feist, B.E., Somers, K.A., Tuttle, V.J., Watson, J.T., Satterthwaite, W.H., 2021. Redistribution of salmon populations in the northeast Pacific Ocean in response to climate. Fish Fish. 22 (3), 503–517.

Sweet, W.V., Kopp, R.E., Weaver, C.P., Obeysekera, J.T.B., Horton, R.M., Thieler, E.R., Zervas, C.E. 2017. Global and regional sea level rise scenarios for the United States. NOAA technical report NOS CO-OPS 83. doi: 10.7289/v5/tr-nos-coops-083.

Sydeman, W.J., Bradley, R.W., Warzybok, P., Abraham, C.L., Jahncke, J., Hyrenbach, K. D., Kousky, V., Hipfner, J.M., Ohman, M.D., 2006. Planktivorous auklet Ptychoramphus aleuticus responses to ocean climate, 2005: Unusual atmospheric blocking? Geophys. Res. Lett. 33 (22).

Thompson, A.R., Schroeder, I.D., Bograd, S.J., Hazen, E.L., Jacox, M.G., Leising, A.L., Wells, B.K., Largier, J.L., Fisher, J.L., Jacobson, K., Zeman, S., Bjorkstedt, E.P., Robertson, R.R., Kahru, M., Georicke, R., Peabody, C.E., Baumgartner, R.R., Lavaniegos, B.E., Miranda, L.E., Gomez-Ocampo, E., Gomez-Valdez, J., Auth, T.R., Daly, E.A., Morgan, C.A., Burke, B.J., Field, J.C., Sakuma, K.M., Weber, E.D., Watson, W., Porquez, J.M., Dolliver, J., Lyons, D., Orben, R.A., Zamon, J.E., Warzybok, P., Jahncke, J., Santora, J.A., Thompson, S.A., Hoover, B., Sydeman, W. J., Melin, S.R., 2019. State of the California Current 2018–19: a novel anchovy regime and a new marine heatwave? CalCOFI Reports 60, 1–65.

Ware, D.M., Thomson, R.E., 2005. Bottom-up ecosystem trophic dynamics determine fish production in the Northeast Pacific. Science 308 (5726), 1280–1284.

Weber, E.D., Auth, T.D., Baumann-Pickering, S., Baumgartner, T.R., Bjorkstedt, E.P., Bograd, S.J., Burke, B.J., Cadena-Ramírez, J.L., Daly, E.A., De La Cruz, M., Dewar, H., Field, J.C., Fisher, J.L., Giddings, A., Goericke, R., Gomez-Ocampo, E., Gomez-Valdes, J., Hazen, E.L., Hildebrand, J., Horton, C.A., Jacobson, K.C., Jacox, M.G., Jahncke, J., Kahru, M., Kudela, R.M., Lavaniegos, B.E., Leising, A., Melin, S.R., Miranda-Bojorquez, L.E., Morgan, C.A., Nickels, C.F., Orben, R.A., Porquez, J.M., Portner, E.J., Robertson, R.R., Rudnick, D.L., Sakuma, K.M., Santora, J.A., Schroeder, I.D., Snodgrass, O.E., Sydeman, W.J., Thompson, A.R., Thompson, S.A., Trickey, J.S., Villegas-Mendoza, J., Warzybok, P., Watson, W., and Zeman, S.M. 2021. State of the California Current 2019–2020: Back to the Future With Marine Heatwaves? Frontiers in Marine Science 8.

Weise, M.J., Costa, D.P., Kudela, R.M., 2006. Movement and diving behavior of male California sea lion (Zalophus californianus) during anomalous oceanographic conditions of 2005 compared to those of 2004. Geophys. Res. Lett. 33 (22).

Wells, B.K., Santora, J.A., Henderson, M.J., Warzybok, P., et al., 2017. Environmental conditions and prey-switching by a seabird predator impact juvenile salmon survival. J. Marine Systems 174, 54–63.

Xiu, P., Chai, F., Curchitser, E.N., et al., 2018. Future changes in coastal upwelling ecosystems with global warming: the case of the California Current System. Sci. Rep. 8, 2866. https://doi.org/10.1038/s41598-018-21247-7.

Zeidberg, L.D., Isaac, G., Widmer, C.L., Neumeister, H., Gilly, W.F., 2011. Egg capsule hatch rate and incubation duration of the California market squid, *Doryteuthis (Loligo) opalescens*: insights from laboratory manipulations. Mar. Ecol. 32, 468–479. https://doi.org/10.1111/j.1439-0485.2011.00445.x.

Zwolinski, J.P., Emmett, R.L., Demer, D.A., 2011. Predicting habitat to optimize sampling of Pacific sardine (*Sardinops sagax*). ICES J. Mar. Sci. 68, 867–879.